Clays and Clay Minerals, Vol. 47, No. 3, 319–328, 1999.

OCCURRENCE OF CLINOPTILOLITE AND MORDENITE IN TERTIARY CALC-ALKALINE PYROCLASTITES FROM SARDINIA (ITALY)

MARIA R. GHIARA,[1] CARMELA PETTI,[1] ENRICO FRANCO,[1] ROBERTO LONIS,[2] SANTINA LUXORO,[2] AND LUCIO GNAZZO[1]

[1] Dipartimento di Scienze della Terra, Università Federico II di Napoli, via Mezzocannone 8, 80134 Napoli, Italy
[2] PROGEMISA Società Sarda Valorizzazione Georisorse, Cagliari, Italy

Abstract—Clinoptilolite and mordenite occur as diagenetic products of medium-grained, moderately welded and poorly sorted pyroclastic flows belonging to the Tertiary calc-alkaline volcanism of Sardinia. Both clinoptilolite and mordenite occur within pyroclastic flows of the same stratigraphic unit. Mordenite frequently occurs in the late volcanic sequences from Anglona area (northern Sardinia). Textural features indicate that zeolites are products of glass alteration. Thin sections show either complete alteration of glassy shards by clinoptilolite and mordenite or unaltered shards with clinoptilolite or mordenite confined to the cineritic matrix. During the zeolitization process, interacting fluids were important in the mobilization and distribution of alkali elements. The compositional variations of clinoptilolite and mordenite within a single sample showed trends that suggest steps in a continuous process probably evolving towards equilibrium conditions.

Key Words—Clinoptilolite, Fluid/Rock Interaction, Mordenite, Opal-CT, Tertiary Pyroclastic Flows.

INTRODUCTION

The nature of the interaction between natural fluids and rocks is fundamental to understand geological processes such as the ocean crust-seawater budget (Crovisier *et al.*, 1987; Jercinovic *et al.*, 1990; Hajash and Bloom, 1991). Glass-water interaction is commonly regarded as a dominant reaction in volcanic rock/water systems, where it largely contributes to mass transfer at an early stage of alteration. During rock-water interaction, differences in the reaction products, crystallization sequences, and reaction kinetics seem to be related to several intensive variables such as interaction times, hydrological system (closed or open), temperature, pH, chemical composition of contact solutions, and starting materials (Boles, 1988; Barth-Wirsching and Holler, 1989; Crovisier *et al.*, 1990, 1992; Ghiara *et al.*, 1993; Daux *et al.*, 1994).

The voluminous Oligo-Miocene pyroclastic flows of Sardinia are very useful to investigate the fluid rock-interaction processes as these rocks were emplaced in volcano-tectonic depressions (Tertiary Sardinian Rift) in the subaerial, lacustrine, and marine environments (Cherchi and Montadert, 1982). Preliminary research on subaerial pyroclastic flows in the Castelsardo basin, northern Sardinia (Ghiara *et al.*, 1995), showed evident transformations (clinoptilolite and smectite) of the glassy components, resulting from intense fluid and glass interactions.

Clinoptilolite and mordenite are widely distributed in nature and were found in post-Jurassic pyroclastic rocks, especially from Tertiary times. These zeolites are usually regarded as "diagenetic" products of glassy rhyolitic fragments (pumices, scories, shards, and vitric ash) crystallized in different geological environments: "closed", saline-lake systems; "open", fresh water-lake or groundwater systems; marine environments; low-grade burial metamorphism; and hydrothermal or hot-spring systems (Iijima and Utada, 1966; Gottardi and Galli, 1985; Ogihara and Iijima, 1990).

In Italy, diagenetic clinoptilolite and mordenite were described at Zovencedo, Vicenza (Alietti and Ferrarese, 1967) and at Ponza island (Passaglia *et al.*, 1995), respectively.

Clinoptilolite and heulandite are isostructural, and are end-members of a continuous solid-solution series (Boles, 1972; Alietti, 1972; Alberti, 1975; Gottardi and Galli, 1985). Conventionally, the compositional boundary of clinoptilolite is where Si/Al > 4.0 and (Na + K) > (Ca + Sr + Ba) (Mason and Sand, 1960; Boles, 1972). The thermal behavior of clinoptilolite and heulandite is different. The clinoptilolite structure is not destroyed after 12 h of heating at 750°C, whereas the heulandite structure is destroyed after 12 h at 450°C (Mason and Sand, 1960; Mumpton, 1960). However, the calcic clinoptilolite structure is destroyed between 450–550°C (Alietti *et al.*, 1977).

Mordenite often coexists with clinoptilolite, suggesting similar conditions of formation. Mordenite shows a Si/Al ratio ranging from 4.2 to 5.9. Mordenite also has Ca from 1.6 to 2.5, Na from 2.0 to 5.0, and K from 0.1 to 0.8 atoms per unit cell (Passaglia, 1975). The very high Si/Al ratio in mordenite produces a high thermal stability. The framework structure shows little change as a result of dehydration, and the mineral is stable to 900°C (Tsitsishvili *et al.*, 1992).

The poorly welded pyroclastic flows belonging to the central and northern Sardinian Rift are studied here

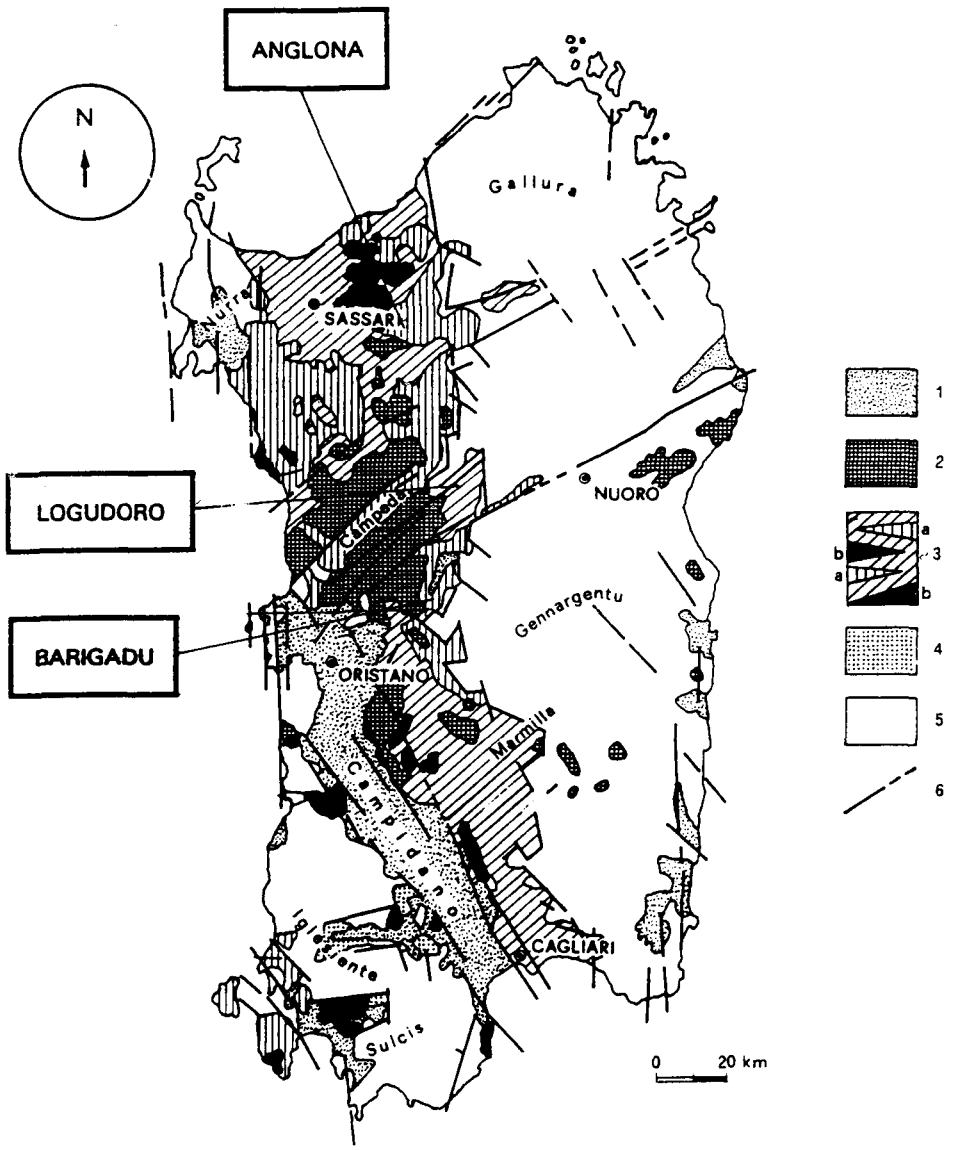

Figure 1. Simplified geological-structural sketch map of Sardinia (modified from Cherchi and Montadert, 1982). (1) Pliocene-Quaternary sediments; (2) Pliocene-Quaternary volcanics; (3) marine sediments and volcanics of Oligo-Miocene age: a) ignimbrites, b) andesites; (4) Cixerri formation; (5) undifferentiated Paleozoic basement and Mesozoic to Eocene covers; (6) Post-Paleozoic main regional faults.

to verify the presence of zeolites previously identified only in the Castelsardo area (Ghiara *et al.*, 1995). A series of representative pyroclastic units from Anglona (northern Sardinia), Logudoro (north-east Sardinia), and Barigadu (central Sardinia) areas (Figure 1) were sampled.

GEOLOGICAL SETTING AND PETROGRAPHY OF PYROCLASTIC FLOWS

The Tertiary calc-alkaline volcanism of Sardinia is characterized by a close field association of many andesitic lava types and strongly acid pyroclastic flows. According to K/Ar radiometric ages, this volcanism started at 32 Ma, with a climax of activity between 24–18 Ma (Beccaluva *et al.*, 1985) with most of the ignimbritic products being generated at this time and affecting the western area of the island. The last calc-alkaline volcanism dates back to 15–16 Ma. Volcanic sequences interbedded with continental and marine sediments are mainly found within the Sardinian Oligocene-Miocene rift ("*fossa tettonica sarda*" of Vardabasso, 1963) which extends 220 km across Sardinia on a NS trend (Cherchi and Montadert, 1982 and references therein). These sequences rarely occur inside

https://doi.org/10.1346/CCMN.1999.0470308 Published online by Cambridge University Press

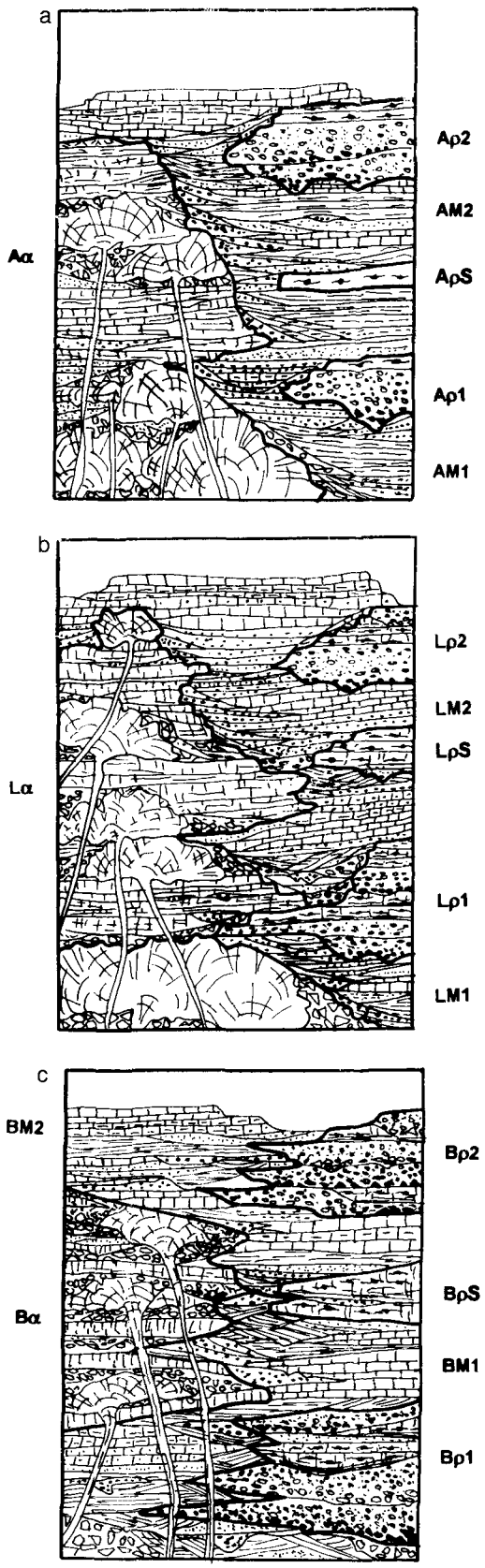

the EW trending minor rift structures (*e.g.*, Cixerri, Funtanazza).

The complex scenario of the Sardinian Rift was recently described as follows: at an early stage in the eastern sector, some sub-basins formed and were filled with Oligocene to Aquitanian sediments and volcanic products. These basins (Carmignani *et al.*, 1994) were related to NE trending sinistral strike-slip movements associated with apenninic collision. Then, during the Burdigalian period, a more pronounced extensional tectonic setting after the counterclockwise rotation of the Sardinian-Corsica palaeoplate led to wider basins on a NW trend (NS main rift) (Assorgia *et al.*, 1995; Carmignani *et al.*, 1994).

New extensive geological surveys in central and northern Sardinia together with radiometric ages (Progemisa, 1990–1994) indicated that the poorly welded pyroclastic flows may be divided into two main cycles separated by an Aquitanian transgression.

←

Figure 2. a) Stratigraphic succession of the sedimentary volcanic sequence in Anglona (Northern Sardinia). Aα: Andesitic and basalt-andesitic lavas and epiclastites (30 ± 1.1 Ma to 17.7 ± 0.8 Ma). AM1: Conglomerates, sandstones, chert limestones, tuffs, marls, and silty clays ranging from fluvial to lacustrine to marine environments (upper Oligocene ?-Aquitanian). Aρ1: Rhyodacitic pyroclastic flows, poorly welded and sometimes rich in pumice and poligenic lithic (21.3 ± 1 Ma). AρS: Eutaxitic and welded rhyolitic flow (19.7 ± 0.5 Ma). AM2: Conglomerates, sandstones, tuffs, limestones, marl limestones, marls, and calcarenites in delta-fluvial to littoral environments (Burdigalian-Serravalian). Aρ2: Poorly welded and pumiceous rhyodactic pyroclastic flows (18.4 ± 1 Ma). b) Stratigraphic succession of the sedimentary volcanic sequence in Logudoro (Northern Sardinia). Lα: Andesitic and basalt-andesitic lavas and epiclastites (30.3 ± 1.5 Ma to 14.3 ± 0.2 Ma). LM1: Conglomerates and sandstones sometimes rich in volcanic components of fluvio-lacustrine environment (upper Oligocene ?-Aquitanian). Lρ1: Rhyodacitic pyroclastic flows, poorly welded, pumice cineritic with vitroclastic texture, sometimes rich in poligenic lithic fragments with interbedded welded rhyolithic flows (23.2 ± 0.8 Ma). LρS: Welded rhyolitic flow pyroclastites. LM2: Conglomerates, sandstones, tuffs, limestones, marl limestones, marls, and calcarenites in delta-fluvial to littoral environment (Burdigalian-Serravalian). Lρ2: Rhyodacitic pyroclastic flows (17.6 ± 0.5 Ma to 16.2 ± 1 Ma). c) Stratigraphic succession of the sedimentary volcanic sequence in Barigadu (Northern Sardinia). Bα: Andesitic and basalt-andesitic lavas and epiclastites BM1: Breccias, conglomerates, sandstones, tuffs, marls, and silted clays, limestones in continental to transitional to litoral environments (upper Oligocene ?-Aquitanian). Bρ1: Poorly welded and pumiceous rhyodacitic pyroclastic flows sometimes rich in poligenic lithic fragments with interbedded welded rhyolithic flows (24.1 ± 0.6 Ma). BρS: Eutaxitic and welded rhyolitic flow. BM2: Conglomerates, sandstones, tuffs, limestones, marl limestones, marls, and calcarenites in delta-fluvial to litoral environments (Burdigalian-Serravalian). Bρ2: Poorly welded rhyodacitic pyroclastic flows, sometimes pumice-rich commonly interbedded with welded rhyolitic pyroclastic flows and local epoclastic levels (19.4 ± 1 Ma).

https://doi.org/10.1346/CCMN.1999.0470308 Published online by Cambridge University Press

Table 1. Mineralogical and petrographic features.

Sample	Locality	Stratigraphic unit[1]	Petrographic type	Phenocryst[2]	Secondary minerals
	Anglona area				
15	S. Maria Coghinas	Aρ1	Rhyodacite	Pl, Bt, Mt, Amp, Qz	Cp, Sm
6233	Concas, Chiaromonti	Aρ2	Rhyodacite	Pl, Bt, Mt, Amp, Qz	Cp, Sm, Op
6333	St.zo Silimbru, Ozieri	Aρ2	Rhyolite	Pl, Bt, Mt, Qz	Mo, Sm, Op
6327	Migaleddu, Ozieri	Aρ2	Dacite	Pl, Bt, Mt, Qz	Mo, Sm
6334	Ozieri l.s.	Aρ2	Dacite	Pl, Bt, Mt, Amp, Qz	Mo, Sm
6331	Mt. Corvos, Ozieri	Aρ2	Rhyolite	Pl, Kf, Bt, Mt, Qz	Mo, Sm
6458	N.ghe Brundette, Ittiri	Aρ2	Rhyodacite	Pl, Kf, Bt, Mt, Qz	Sm
	Logudoru area				
6753	Sas Contones, Anela	Lρ1	Rhyodacite	Pl, Bt, Qz, Mt	Cp, Sm
5616	Mt. Abile, Bonorva	Lρ2	Rhyodacite	Pl, Kf, Bt, Mt, Qz	Sm
5636	Pedrosu, Ittireddu	Lρ2	Rhyodacite	Pl, Kf, Bt, Mt, Px, Qz	Sm
5639	Sa Pattada, Ittireddu	Lρ2	Rhyodacite	Pl, Kf, Bt, Mt, Amp, Qz	Sm
5617	Mt. Abile, Bonorva	Lρ2	Rhyodacite	Pl, Bt, Mt, Qz	Cp
5615	Mt. Niedda, Bonorva	Lρ2	Rhyodacite	Pl, Bt, Mt, Anf, Qz	Cp, Sm
5608	Sa Chea de Sainu, Ozieri	Lρ2	Rhyolite	Pl, Kf, Bt, Mt, Qz	Cp, Sm
5614	Sa Fraigada, Bonorva	Lρ2	Rhyodacite	Pl, Bt, Mt, Qz	Mo, Op
6921	Case del Vento, Bosa	Lρ2	Rhyodacite	Pl, Bt, Mt, Amp, Qz	Cp, Sm
	Barigadu area				
6504	Salto di Lochele, Olzai	Bρ1	Rhyolite	Pl, Kf, Bt, Mt, Amp, Qz	Cp, Sm
6241	Paule Lutturu, Samugheo	Bρ1	Rhyolite	Pl, Bt, Mt, Amp, Qr	Cp, Sm
6314	Azzapulau, Busachi	Bρ1	Rhyodacite	Pl, Bt, Mt, Px, Qz	Mo, Sm
6310	Nurache, Samugheo	Bρ1	Rhyolite	Pl, Kf, Bt, Mt, Amp, Qz	Sm
6268	Paule Lutturu, Samugheo	Bρ1	Rhyolite	Pl, Kf, Bt, Mt, Qz	Cp, Sm
6269	Paule Lutturu, Samugheo	Bρ1	Rhyolite	Pl, Kf, Bt, Mt, Qz	Sm, Ana, Qz
6304	Laccu e Mare, Busachi	Bρ1	Rhyolite	Pl, Kf, Bt, Mt, Amp, Qz	Cp, Sm
6303	F. Mannu, Samugheo	Bρ1	Ryodacite	Pl, Mt, Bt, Qz	Sm, Ana, Qz
6306	F. Mannu, Samugheo	Bρ1	Rhyolite	Pl, Kf, Bt, Mt, Qz	Mo, Sm, Qz
6302	F. Mannu, Samugheo	Bρ1	Rhyolite	Pl, Kf, Bt, Mt, Amp, Qz	Cp, Sm
6500	Bapantari, Bidoni	Bρ2	Rhyodacite	Pl, Kf, Bt, Qz	Cp, Sm
6272	Cuglieri l.s.	Bρ2	Rhyolite	Pl, Kf, Bt, Mt, Amp, Qz	Cp, Op
6271	Cuglieri l.s.	Bρ2	Rhyodacite	Pl, Kf, Bt, Mt, Amp, Qz	Mo, Op

[1] Stratigraphic units as in Figure 2.

[2] Pl = plagioclase, Bt = biotite, Kf = K-feldspar, Qz = quartz, Mt = magnetite, Amp = amphibole, Cp = clinoptilolite, Mo = mordenite, Sm = smectite, Ana = analcime, Op = opal-CT.

Schematic Oligo-Miocene stratigraphies for the volcanic sequences in central and northern Sardinia are given in Figure 2. The explosive activity of the two cycles is both due to column collapse of ashes or pumice flows and welded lava-like ignimbrites. The pyroclastic flows are consistently interbedded with continental and marine sediments. In the continental and marine clastic rocks, volcaniclastic components are always abundant.

Petrographic features of poorly welded pyroclastic flows are summarized in Table 1. Pyroclastic flows are medium-grained, moderately welded, and poorly sorted. Large lithic clasts were frequently observed. Laminated epiclastic levels are frequently interbedded with pyroclastic units. The rocks show a porphyroclastic texture with a porphyritic index ranging from 20 to 35%. The flattening of glass fragments and pumice produced a slightly eutaxitic texture at the base of the pyroclastic unit. A vitroclastic texture is well preserved in all samples. Strongly zoned plagioclases (An_{70-30}), corroded quartz, and subordinate biotite laths are the main phenocrystic phases. K-feldspar is significant only in some units, whereas it is a minor constituent in others. Plagioclase and K-feldspar are normally fresh whereas biotite is slightly chloritized. Common accessory phases are opaques and apatite. Phenocryst assemblages and the composition glass indicate that ignimbrites range from rhyodacite to rhyolite. Xenolithic components mainly consist of angular fragments of "andesitic" rocks and rounded clasts of crystalline basement.

Glassy shards and pumices, in thin sections, often show a variable degree of alteration leading to fine-grained colorless aggregates. Secondary minerals appear in two contrasting crystal-growth forms ranging from euhedral to anhedral grains. Clinoptilolite is easily recognizable due to its tabular crystal habit, weak birefringence, low refractive indices, and near parallel extinction in longitudinal sections. Crystals typically nucleate on the rim of a shard, and tend to grow inward (Figure 3a). Mordenite, in contrast, shows typical

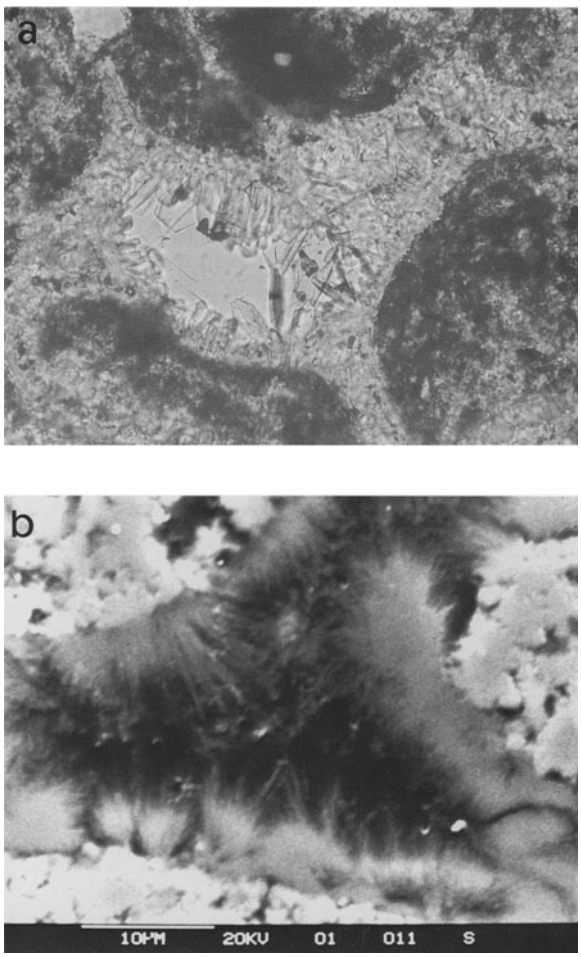

Figure 3. Zeolitized shards in pyroclastic flow from northern Sardinia. a) 250 × plane-polarized light, shard altered to clinoptilolite, note the radial arrangement; b) SEM micrograph of shard altered to fibrous mordenite aggregates.

thin and curved fibers, arranged as fibrous or felted aggregates (Figure 3b).

MATERIAL AND METHODS

The material investigated was collected in the central and northern part of the main Sardinian rift (Italy). Only samples that were representative of extensive, poorly welded pyroclastic flows were sampled (Figure 2). About 1 kg of samples was collected in the central part of each deposit (Table 1).

Zeolites were identified by means of X-ray diffraction (XRD) analysis using a Philips PW 1730 X-ray diffractometer (40 kV, 30 mA) with Ni-filtered Cukα radiation. Samples were heated for 12 h at 450, 550, 750, 800, and 900°C to determine the thermal stability of clinoptilolite and mordenite of the zeolite-enriched fraction. Chemical composition was determined by electron microprobe analysis (Bence and Albee, 1967) using a Cameca Sx50 microprobe operating at an acceleration voltage of 15 kV, a beam current of 15 nÅ, and a spot size of 10 μm. Precision of most elements is better than ±2% but an error of ±5–10% may exist for Na.

A Stereoscan Cambridge 250 TP scanning electron microscope (SEM) was used to obtain crystal-habit data of authigenic minerals. XRD of glycolated samples was performed on oriented clay-mineral fractions. To better identify analcime, differential thermal analysis (DTA), thermogravimetric analysis (TG), and differential thermogravimetric analysis (DTG) were performed using a NETZSCH Geratebau GMBH instrument and a heating rate of 10°C/min between 20–1000°C. Opal-CT was determined by infrared spectroscopy (Perkin-Elmer 457).

RESULTS

From microscope and XRD data the following main features on secondary minerals were observed: most ignimbrites contain zeolites associated with clay minerals; opal-CT and euhedral crystal quartz occur as newly-formed minerals; clinoptilolite is the most widespread zeolite found, followed by mordenite; analcime occurs rarely only in a few samples; textural evidence indicates that the zeolites form, as commonly observed elsewhere, from the alteration of glass.

Petrographic observations of pyroclastites confirmed that alteration is variable. In some thin sections, complete alteration of glassy shards to clinoptilolite (*e.g.*, samples 15, 6233, 5615, 6241) is observed whereas in others, the clinoptilolite is confined mostly to the cineritic matrix (*e.g.*, samples 5617, 6268). XRD patterns taken of the heated samples (Figure 4) at room temperature show the thermal behavior of clinoptilolite (*e.g.*, sample 5617) and mordenite (*e.g.*, sample 5614). Clinoptilolite crystal-habit was observed by SEM and Figure 5 shows a well-developed crystal habit, similar to that reported by Mumpton and Ormsby (1976). In coarse-grained assemblages, clinoptilolite laths reach 30 μm along the *c* axis and nearly 5 μm in thickness. The radial arrangement of clinoptilolite assemblages is observed.

Representative electron microprobe analyses of clinoptilolites are given in Table 2. Framework-cation contents are plotted in Figure 6. Alkaline and alkaline-earth elements range from 1.8 (sample 6302) to 3.3 (samples 5615, 6504) atoms and from 1.25 (sample 6504) to 2.0 (sample 6302) atoms per unit cell, respectively. Si/Al ratio is quite constant (ranges from 4.6 to 4.7), the Na/K ratio ranges from 0.43 (sample 6500) to 1.5 (sample 6504), and (Na + K) > (Ca + Mg) for all samples except 6303. Therefore, according to Bole (1972), the samples are classified as clinoptilolites and sample 6302 is classified as Ca rich-clinoptilolite. All samples persist after heating at 800°C for 12 h and hence, they are classified as clinoptilolite also based on the scheme by Mumpton (1960).

https://doi.org/10.1346/CCMN.1999.0470308 Published online by Cambridge University Press

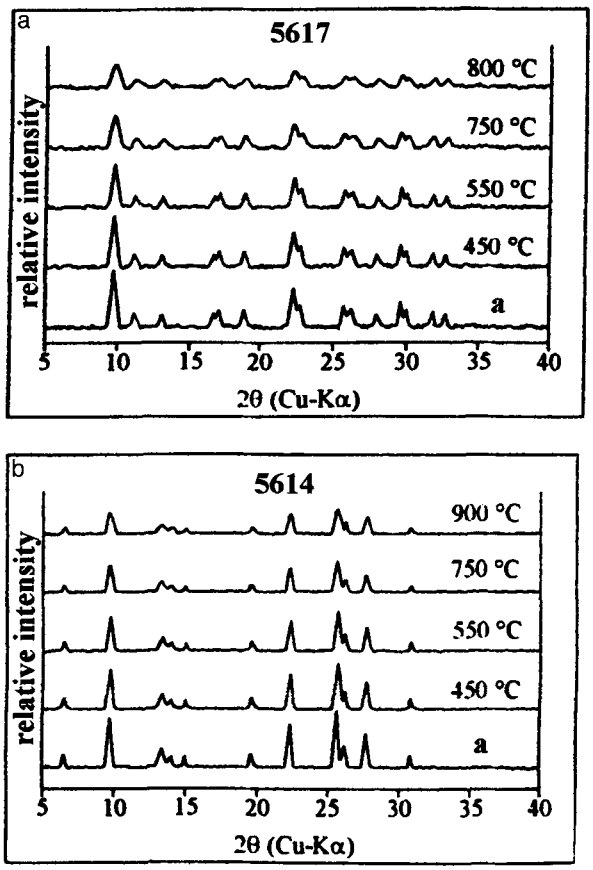

Figure 4. Comparison of diffraction patterns of selected clinoptilolite (samples 5617 unit Lρ2) and mordenite (samples 5614 unit Lρ2) before heating (a) and heat-treated at different temperatures.

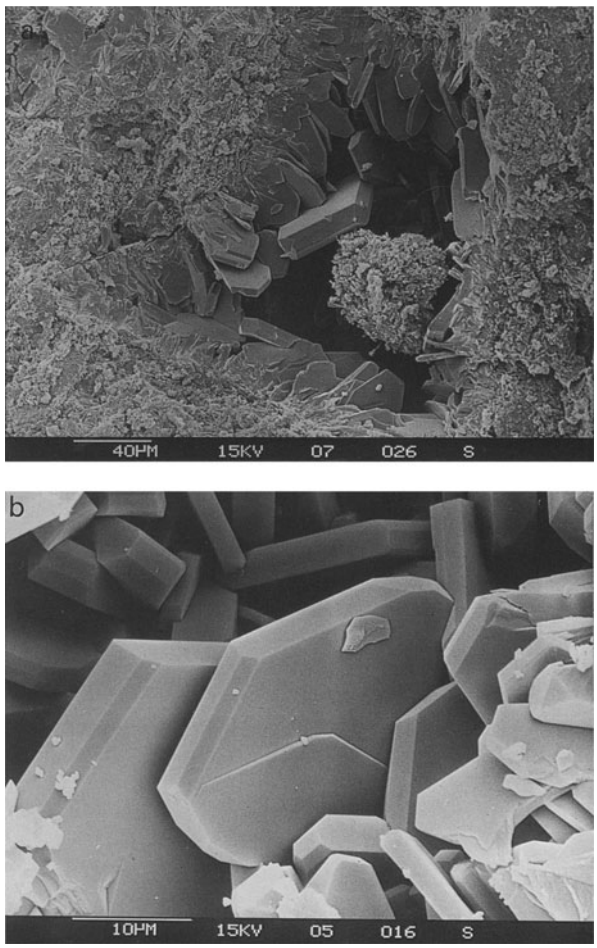

Figure 5. SEM images of clinoptilolite from pyroclastic flow from Sardinia. a) complete alteration of shard into clinoptilolite; b) detail of a), showing the characteristic monoclinic symmetry of the clinoptilolite laths.

Both X-ray and microscopic data indicate that mordenite abundance varies, but generally less than clinoptilolite. Like clinoptilolite, some thin sections showed a complete alteration of both glassy shards and cineritic matrix (*e.g.*, samples 5614, 6327, 6331) whereas others showed that mordenite is exclusively contained in the cineritic matrix (*e.g.*, samples 6303, 6271). Figure 7 shows that the mineral occurs typically as thin curved fibers, occasionally in felted and/or radial aggregates similar to those reported by Mumpton and Ormsby (1976) and Tsitsishvili *et al.* (1992).

In mordenite samples (Table 3), Si/Al ratios range from 4.58 to 5.11, Na is greater than both Ca and K which range from 1.55 to 2.12 atoms and from 0.58 to 2.01 atoms, respectively. Plotted in the (Ca + Mg)-Na-K diagram (Figure 8), the samples fall inside the field for mordenites (Tsitsishvili *et al.*, 1992) except for sample 6331, which is close to diagenetic mordenites (Passaglia *et al.*, 1995).

The secondary minerals, opal-CT and quartz are the most common. Quartz forms as well-formed crystals in small cavities or finely distributed in cineritic matrix. Opal-CT occurs as radial spherulites (Figure 9).

Opal-CT (Jones and Segnit, 1971) was identified by XRD by using the peaks at 20–22 °2θ (Segnit *et al.*, 1970; Florke *et al.*, 1975). The infrared spectra of opal-CT (KBr pellets) is characterized by broad-band absorption centered at ~3450 cm^{-1} (O-H stretching), by two bands centered at ~1100 and 798 cm^{-1} (Si-O stretching) and by a narrow band at ~440 cm^{-1} (Si-O bending vibrations). Infrared absorption spectra were in good agreement with those reported by Graetsch (1994).

XRD analyses of nearly all samples showed a dioctahedral smectite in the cineritic mass (Figure 10) with $d(001)$ varying from ~12 to 15 Å. The $d(001)$ is equal to 16.67 Å when treated with ethylene glycol for 1 h at 60°C.

DISCUSSION AND CONCLUSION

Our investigations of Tertiary poorly welded pyroclastic flows of Anglona, Logudoro, and Barigadu ar-

https://doi.org/10.1346/CCMN.1999.0470308 Published online by Cambridge University Press

Table 2. Selected microprobe analysis of clinoptilolite from pyroclastic flows of Sardinia.

Sample	15 [6][1]	5615 [10]	6302 [10]	6500 [8]	6504 [4]
SiO_2	67.53 (2.03)[2]	67.68 (1.58)	69.71 (0.93)	69.41 (0.78)	71.02 (0.54)
Al_2O_3	12.15 (0.49)	12.55 (0.30)	12.53 (0.34)	12.46 (0.26)	12.70 (0.43)
Fe_2O_3	0.11 (0.52)	0.04 (0.03)	0.05 (0.04)	0.05 (0.06)	0.07 (0.06)
MgO	0.84 (0.15)	0.75 (0.05)	1.19 (0.11)	0.99 (0.07)	0.76 (0.11)
CaO	2.10 (0.35)	1.87 (0.10)	2.63 (0.09)	2.45 (0.16)	1.74 (0.14)
Na_2O	1.25 (0.43)	1.34 (0.19)	0.70 (0.10)	0.84 (0.11)	2.45 (0.24)
K_2O	2.90 (0.23)	3.91 (0.35)	2.25 (0.23)	2.92 (0.22)	2.46 (0.15)
Si	29.79	29.62	29.81	29.79	29.81
Al	6.32	6.47	6.32	6.31	6.28
Fe^{3+}	0.04	0.01	0.02	0.02	0.02
Mg	0.55	0.49	0.76	0.63	0.47
Ca	0.99	0.87	1.20	1.12	0.78
Na	1.07	1.14	0.58	0.69	1.99
K	1.63	2.18	1.23	1.60	1.32
[3]E%	9.10	6.81	9.58	8.29	7.75
Si/Al	4.71	4.58	4.72	4.72	4.74
(Na + K)/(Ca + Mg)	1.75	2.44	0.92	1.31	2.64

[1] Number of analyses for each sample. The unit formula is calculated on the basis of 72 oxygens.
[2] Estimated standard deviations are given to the right of each number.
[3] $E\% = (Al + Fe^{3+}) - [(Na + K) + 2(Mg + Ca)]/(Al + Fe^{3+}) \times 100$ from Gottardi and Galli, 1985.

eas (Sardinia, Italy) showed that most are generally altered to clinoptilolite, mordenite, and smectite. Secondary minerals include quartz and opal-CT. The textural relationships, inferred by plane polarized light and SEM investigations, suggest that zeolites are mainly alteration products related to partial or complete dissolution of glassy components (shards and vitric ash) of rhyolitic ignimbrites and opal-CT aggregates are clearly a late-phase filling small cavities or overgrowth on zeolites. Both secondary mineral assemblages and textural features are consistent with a hydrothermal alteration process defined by Henley and Hellis (1983). This process includes: mineral and glass dissolution, new mineral crystallization and, especially in the porous zones of ignimbrites, vapor-phase deposition and ion-exchange reactions.

Cliniptilolite (Table 1) shows wide variations in exchangeable cation content, whereas the Si/Al ratio is less variable. Generally the (Ca + Mg)-K-Na diagram defines a trend ranging from low (Ca + Mg) minerals (*e.g.*, samples 5615, 6504) to samples rich in (Ca + Mg) (*e.g.*, sample 6302). Furthermore, in each rock sample, clinoptilolite shows compositional variations consistent with the general trend illustrated in Figure 6, even in crystals from the same shards.

The high thermal stability of silica-rich zeolites is consistent with chemistry. Clinoptilolite begins to decompose above 800°C, whereas mordenite is stable to

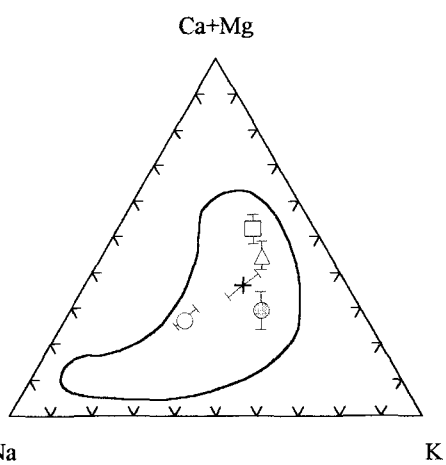

Figure 6. The (Ca + Mg)-Na-K relationship for clinoptilolite. Symbols: □ sample 6302 unit Bρ2, ● sample 5615 unit Lρ2, ○ sample 6504 unit Bρ1, + sample 15 unit Aρ1, △ sample 6500 unit Bρ2. The lines represent the compositional variation within each sample analyzed.

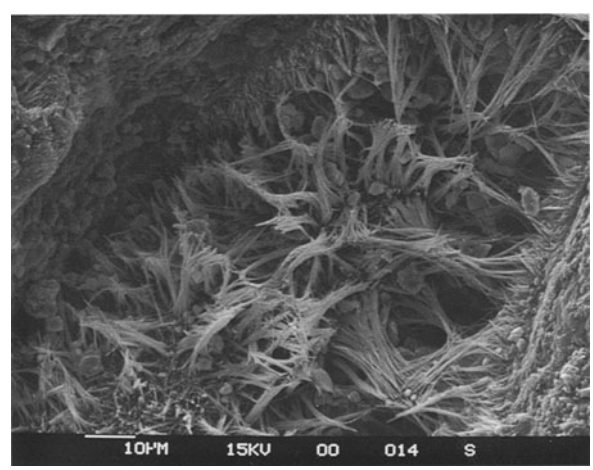

Figure 7. SEM image of mordenite replacing glassy shards from pyroclastic flows from Sardinia.

https://doi.org/10.1346/CCMN.1999.0470308 Published online by Cambridge University Press

Table 3. Representative microprobe analysis of mordenite from pyroclastic flows of Sardinia.

Sample	5614 [7][1]	6327 [8]	6331 [5]
SiO_2	71.36 (1.05)[2]	67.33 (0.06)	67.25 (3.46)
Al_2O_3	11.85 (0.44)	12.48 (0.44)	11.78 (0.36)
Fe_2O_3	0.40 (0.30)	0.24 (0.19)	0.02 (0.02)
MgO	0.28 (0.36)	0.19 (0.08)	0.02 (0.02)
CaO	3.03 (0.13)	3.39 (0.11)	2.45 (0.10)
Na_2O	2.51 (0.28)	2.19 (0.33)	2.00 (0.05)
K_2O	0.81 (0.38)	1.28 (0.33)	2.60 (0.25)
Si	40.11	39.45	39.90
Al	7.85	8.62	8.24
Fe^{3+}	0.17	0.11	0.01
Mg	0.23	0.17	0.02
Ca	1.81	2.12	1.55
Na	2.73	2.48	2.30
K	0.58	0.96	2.01
[3]E%	7.62	8.17	9.68
Si/Al	5.11	4.58	4.84
Ca/K	3.12	2.21	0.77
Ca/Na	0.66	0.85	0.67

[1] Number of analysis for each sample.
[2] Estimated standard deviations are given to the right of each number.
[3] E% = $(Al + Fe^{3+}) - [(Na + K) + 2(Mg + Ca)]/(Al + Fe^{3+}) \times 100$ from Gottardi and Galli, 1985.

900°C (Figure 4). The highest thermal stability of mordenite is related to its high Si/Al ratio.

The chemical compositions of glasses, clinoptilolite, and mordenite (Table 4), renormalized using an anhydrous standard cell (Barth, 1952), show that during the zeolitization process a depletion of alkaline elements and a slight increase in Ca and Mg occurs. Since the chemistry of the initial glass is similar for both clinoptilolite and mordenite crystallization, clinoptilolite clearly selectively concentrates K and mordenite

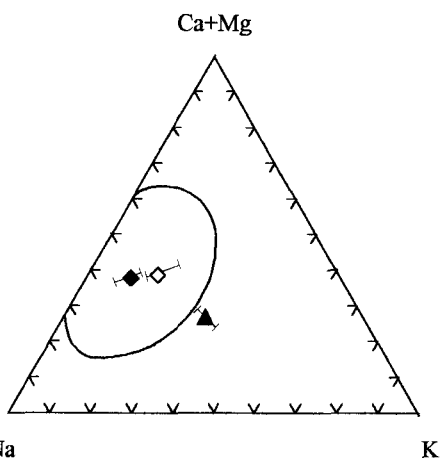

Figure 8. The (Ca + Mg)-Na-K diagram of mordenite. Symbols: ▲ sample 6331 unit Aρ2, ◆ sample 5614 unit Lρ2, ◇ sample 6327 unit Aρ2. The lines represent the compositional variation within each sample analyzed.

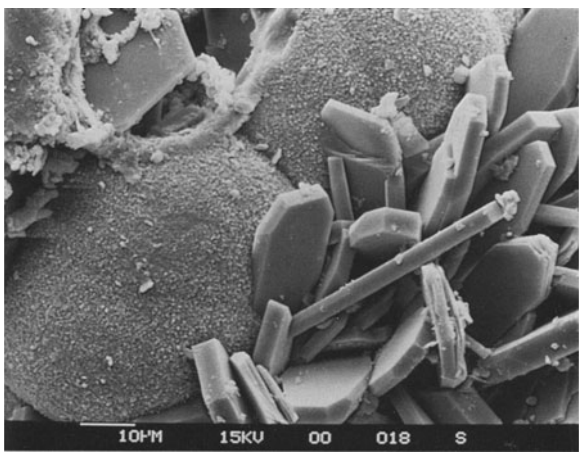

Figure 9. SEM image of the textural relationships of clinoptilolite and opal-CT lepispheres from pyroclastic flows from Sardinia.

concentrates Na. In fact, the average Na content (Table 4) for glass 1 is 6.91, but the average Na content in clinoptilolite is 1.93 atoms (except for sample 6504). In glass 2, the average Na content is 7.37 atoms and this decreases to 4.16 in mordenite. In contrast, the average K value is 7.40 atoms in glass 1 and this decreases to 3.52 atoms in clinoptilolite and from 6.81 to 1.3 (except for sample 6331) in the mordenite samples. These trends may be due to several factors, such as interacting fluid speciation (total dissolved salt, pH, halogen content) (Ghiara and Petti, 1996), absolute temperature (Seyfried and Bischoff, 1979; Thornton and Seyfried, 1985), and the thermal history of the glass (Shiraki and Iiyama, 1990). Figure 11 shows that in clinoptilolite the Ca/K ratio is quite constant whereas the Ca/Na ratio is variable. In mordenite, the Ca/Na ratio is nearly constant and the Ca/K ratio varies greatly. This means that clinoptilolite is stable with

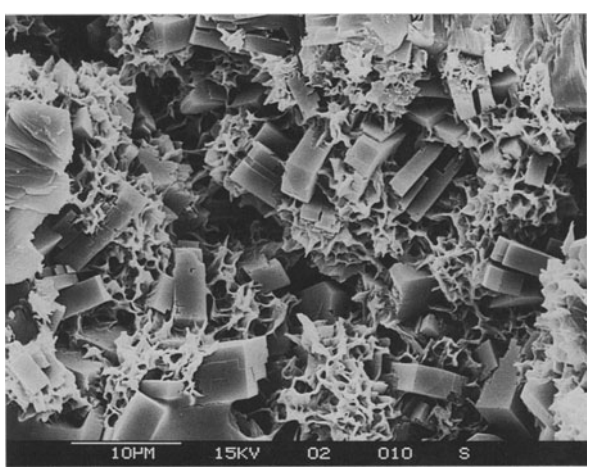

Figure 10. SEM image of smectite with clinoptilolite from pyroclastic flow of Sardinia.

https://doi.org/10.1346/CCMN.1999.0470308 Published online by Cambridge University Press

Table 4. Anhydrous (Barth) standard cell content (atoms) of unalterated glasses (Glass 1; Glass 2), clinoptilolite (samples 15,5615,6302,6504,6500) and mordenite (samples 6331,6327,5614). The unit formula is calculated on the basis of 160 oxygens.

Sample	Glass 1	15	5615	6302	6504	6500	Glass 2	6331	6327	5614
Si	64.44	66.16	65.83	66.23	66.21	65.83	64.18	66.44	65.57	66.78
Al	14.86	14.03	14.34	14.04	13.96	14.07	15.00	13.72	14.27	13.08
Fe^{3+}	0.04	0.06	0.03	0.04	0.06	0.09	0.05	0.02	0.20	0.33
Mg	0.33	1.22	1.04	1.68	1.05	1.43	0.25	0.05	0.28	0.39
Ca	1.13	2.19	1.97	2.67	1.73	2.48	1.51	2.58	3.51	3.02
Na	6.91	2.37	2.51	1.30	4.42	1.55	7.37	3.84	4.11	4.55
K	7.40	3.63	4.79	2.73	2.93	3.59	6.81	3.35	1.59	0.96

appropriate amounts of K and mordenite is stable with appropriate amounts of Na. As demonstrated by experimental studies on zeolite formation (Barth-Wirsching and Höller, 1989; Ghiara *et al.*, 1993; Ghiara and Petti, 1996), the interaction of glass with solutions of different composition will lead to different assemblages. At a given temperature and reaction time, different assemblages were synthesized from rhyolitic glass and NaOH, KOH solutions, or deionized water (Barth-Wirsching and Höller, 1989). In experiments with 0.01 N NaOH solution, mordenite, analcime, alkali feldspar, and quartz formed; clinoptilolite, alkali feldspar, and quartz were synthesized from 0.01 N KOH; and clinoptilolite, mordenite, and alkali feldspar occurred from experiments with deionized water.

From the above results, it is inferred that the zeolitization process of pyroclastic flows is a regional process, suggesting that there is no connection between zeolitization and the local geological environment. Therefore, it is possible to exclude geological environments related to local geothermal fields (*e.g.*, Yellowstone Park, Wairaki) or to massive fluid circulations related to particular tectonic lineaments. We hypothize that the minerogenetic agents were of regional scale. According to experimental data from the literature, the interacting fluids are probably percolating groundwaters or trapped water-gas mixtures of ignimbrites. This latter possibility would produce spherulitic aggregates of silica minerals.

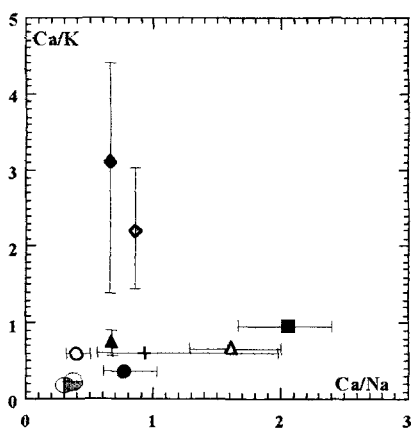

Figure 11. The Ca/Na *vs.* Ca/K ratios of analyzed zeolites showing the clinoptilolite and mordenite trends (for symbols see Figures 6 and 8). Averaged micro-analysis of unalterated shards of two pyroclastic flows are also plotted (◒ glass 1; ◑ glass 2). Note the position of glassy shards with respect to the two trends. The lines represent the compositional variation within each sample analyzed.

ACKNOWLEDGMENTS

Special thanks to A. Cundari who made useful suggestions for improving the paper. We thank S. Guggenheim, J. Honnorez, A. M. Karpoff, and an anonymous referee for critical reading of the final manuscript. M. Sarracino (Centro Studi per il Quaternario el'Evoluzione Ambientale CNR, Roma), A. Canzanella (Dipartimento di Scienze della Terra, Università Federico II Napoli), A. Ibba (Dipartimento di Scienze della Terra, Università di Cagliari), and A. Ambu (Progemisa, Cagliari) are gratefully thanked for help in microprobe, electron microscopy analysis, and thin section preparation, respectively. This research was performed with grants from the Italian C.N.R. No. 9601720.CT11.

REFERENCES

Alberti, A. (1975) The crystal structure of two clinoptilolites. *Tschermaks Mineraogische und Petrographische Mitteilngen*, **22,** 25–37.

Alietti, A. (1972) Polymorphism and crystal-chemistry of heulandites and clinoptilolites. *American Mineralogist*, **57,** 1448–1462.

Alietti, A. and Ferrarese, G. (1967) Clinoptilolite, Na-montmorillonite e ossidi di manganese in una formazione sedentaria a Zovencedo (Vicenza). *Mineralogical et Petrografica Acta*, **13,** 119–138.

Alietti, A., Brigatti, M.F., and Poppi, L. (1977). Natural Ca-rich clinoptilolites (heulandite of group 3): New data rewiew. *Neues Jahrbuch für Mineralogie Monatshefte*, **H11,** 493–501.

Assorgia, A., Balogh, K., Lecca, L., Ibba, A., Porcu, A., Secchi, F., and Tilocca, G. (1995) Volcanological characters and structural context of Oligo-Miocene volcanism successions from central Sardinia (Italy). *Accademia Nazionale delle Scienze Atti Convonvegni Rapporti Alpi-Appennino*, 397–424.

Barth, T.F.W. (1952). *Theoretical Petrology, a Textbook on the Origin and Evolution of Rocks*. Wiley, New York, 398 pp.

Barth-Wirsching, U. and Holler, H. (1989) Experimental studies on zeolite formation conditions. *European Journal of Mineralogy*, **1,** 489–506.

Beccaluva, L., Civetta, L., Macciotta, G., Ricci, C.A. (1985) Geochronology in Sardinia: Results and problems. *Rendi-*

conti Società Italiana di Minealogia e Petrografia, **40,** 57–72.

Bence, A.E. and Albee, A.L. (1967) Empirical correction factors for the electron microanalysis of silicates and oxides. *Journal of Geology*, **76,** 382–403.

Boles, J.R. (1972). Composition, optical properties, cell dimensions and thermal stability of some heulandite group zeolites. *American Mineralogist*, **57,** 1463–1493.

Boles, J.R. (1988) Occurrences of natural zeolites. Present status and future research. In *Occurrence, Properties and Utilization of Natural Zeolites*. D. Kallo and H.S. Sharry, eds., Akademiai Kiadò, Budapest, 3–18.

Carmignani, L., Barca, S., Disperati, L., Fantozzi, P., Funedda, A., Oggiano, G., and Pasci, S. (1994) Tertiary compression and extension in Sardinia Basement. *Bollettino di Geofisica Teorica ed Applicata*, **36,** 45–62.

Cherchi, A. and Montadert, L. (1982) The Oligo-Miocene rift of Sardinia and early history of the western Mediterranean basin. *Nature*, **298,** 736–739.

Crovisier, J.L., Honnorez, J., and Eberhart, J.P. (1987) Dissolution of basaltic glass in seawater: Mechanism and rate. *Geochimica et Cosmochimica Acta*, **51,** 2977–2990.

Crovisier, J., Atassi, H., Daux, V., and Eberhart, J.P. (1990) Hydrolyse d'un vere basaltique tholéiitique à 60°C. Dissolution sélective pui congruente par élévation de pH. *Comptes Rendus de l'Académie des Sciences de Paris, France*, **310 II,** 941–946.

Crovisier, J.L., Honnorez, J., Fritz, B., and Petit, J.C. (1992). Dissolution of subglacial volcanic glasses from Iceland: Laboratory study and modelling. *Applied Geochemistry Supplemental Issue*, **1,** 55–81.

Daux, V., Crovisier, J.L., Hemond, C., and Petit, J.C. (1994) Geochemical evolution of a basaltic rock submitted to weathering: Fate of the major elements rare earth elements and thorium. *Geochimica et Cosmochimica Acta*, **58,** 4941–4954.

Florke, O.W., Jones, J.B., and Segnit, E.R. (1975) Opal-CT crystals. *Neues Jahrbuch für Mineralogie Monatshefte*, 369–377.

Ghiara, M.R. and Petti, C. (1996) Chemical alteration of volcanic glasses and related control by secondary minerals: Experimental studies. *Aquatic Geochemistry*, **1,** 329–354.

Ghiara, M.R., Franco, E., Petti, C., Stanzione, D., and Valentino, G.M. (1993) Hydrothermal interaction between basaltic glass, deionized water and seawater. *Chemical Geology*, **104,** 125–138.

Ghiara, M.R., Pett, C., Franco, E., Luxoro, S., and Gnazzo, L. (1995) Diagenetic clinoptilolite from pyroclastic flows of northern Sardinia. In *Proceedings III Convegno Nazionale Scienza e Tecnologia delle Zeoliti*, R. Aiello, ed., Cetraro, Italy, 349–353.

Gottardi, G. and Galli, E. (1985) *Natural Zeolites*. Springer Verlag, Berlin, 409 pp.

Graetsch, H. (1994) Structural characteristics of opaline and microcrystalline silica minerals. In *Silica Physical Behavior, Geochemistry, and Materials Applications*, P.J. Heaney, C.T. Prewitt, and G.U. Gibbs, eds., Mineralogical Society of America, Washington, DC, **29,** 211–232.

Hajash, A. and Bloom, M.A. (1991) Marine diagenesis of feldspathic sand: A flow-through experimental study at 200°C 1 kbar. *Chemical Geology*, **89,** 359–377.

Henley, R.W. and Hellis, A.J. (1983) Geothermal systems ancient and modern: A geochemical review. *Earth Science Reviews*, **19,** 1–50.

Iijima, A. and Utada, M. (1966). Zeolites in sedimentary rocks with reference to the depositional environments and zonal distribution. *Sedimentology*, **7,** 327–357.

Jercinovic, M.J., Keil, K., Smith, M.R., and Schmitt, R.A. (1990). Alteration of basaltic glasses from north-central Brtish Columbia, Canada. *Geochimica et Cosmochimica Acta*, **54,** 2679–2696.

Jones, J.B. and Segnit, E.R. (1971). The nature of opal. I. Nomenclature and constituent phases. *Journal of the Geology Society of Australia*, **18,** 57–68.

Mason, B. and Sand, L.B. (1960) Clinoptilolite from Patagonia. The relationship between clinoptilolite and heulandite. *American Mineralogist*, **45,** 341–350.

Mumpton, F.A. (1960) Clinoptilolite redefined. *American Mineralogist*, **45,** 351–369.

Mumpton, F.A. and Ormsby, W.C. (1976) Morphology of zeolites in sedimentary rocks by scanning electron microscopy. In *Natural Zeolites Occurrence, Properties, Uses*, L.B. Sand and F.A. Mumpton, eds., 113–132.

Ogihara, S. and Iijima, A. (1990). Exceptionally K-rich clinoptilolite-heulandite group zeolites from three offshore boreholes off northern Japan. *European Journal of Mineralogy*, **2,** 819–826.

Passaglia, E. (1975). The crystal chemistry of mordenites. *Contributions to Mineralogy and Petrology*, **50,** 65–77.

Passaglia, E., Artioli, G., Gualtier, I.A., and Carnevali, R. (1995) Diagenetic mordenite from Ponza, Italy. *European Journal of Mineralogy*, **7,** 429–438.

Progemisa (1990–1994) Ricerca mineraria di base. Convenzioni MICA-EMSa Vucaniti terziarie della Sardegna Aria 1 2 e 3. Ministero dell'Industria, Roma.

Segnit, E.R., Anderson, C.A., and Jones, J.B. (1970) A scanning microscope study of the morphology of opal. *Serch*, **1,** 349–351.

Seyfried, W.E. and Bischoff, J.L. (1979) Low temperature basalt alteration by seawater: An experimental study at 70°C and 150°C. *Geochimica et Cosmochimica Acta*, **43,** 1937–1947.

Shiraki, R. and Iiyama, J.T. (1990) Na-K ion exchange reaction between rhyolitic glass and (Na, K)Cl aqueous solution under hydrothermal conditions. *Geochimica et Cosmochimica Acta*, **54,** 2923–2931.

Thornton, E.C. and Seyfried, W.E. (1985) Sediment-seawater interaction at 200 and 300°C, 500 bars pressure: The role of sediment composition in diagenesis and low grade metamorphism of marine clay. *Geological Society of America Bulletin*, **96,** 1287–1295.

Tsitsishvili, G.V., Andronikashvili, T.G., Kirov, G.N., and Filizova, L.D. (1992) *Natural Zeolites*. Ellis Harwood Ltd, London, 295 pp.

Vardabasso, S. (1963) Die ausseralpine taphrogenese in Kaledonish-variszisch konsolidierten sardischen vorlande. *Sonderdruck aus der Geologischen Rundschau band*, **53,** 613–630.

(Received 6 March 1998; accepted 27 October 1998; Ms. 98-032)